

# Rock Physics simulations using core data to estimate the stiffness tensor in Vaca Muerta organic-rich mudrock

SEG Symposium, Beneath the Surface: Innovations in  
Geoscience. Celebrate the legacy of Sven Treitel, June  
19-20 2025

**Juan E. Santos,**

Universidad de Buenos Aires (UBA), Argentina, Hohai University, Nanjing,  
China and Purdue University, Indiana, USA.

In collaboration [Sanchez Camus \(Solaer Ingemiería, UNLP\)](#), [P. M. Gauzellino \(UNLP\)](#) [G. B. Savioli \(UBA\)](#) and [J. Ba \(Hohai University\)](#)

July 3, 2025

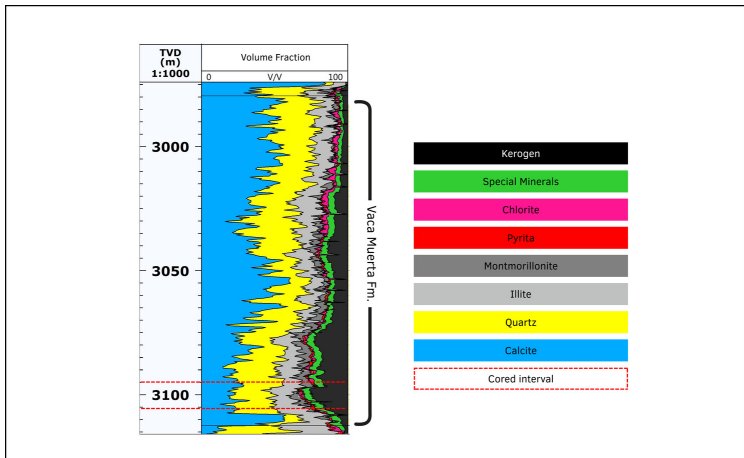
# characterization of ultra-low permeability, organic-rich mudrock reservoirs. I

- This work presents a methodology to characterize and analyze the lower section of the Vaca Muerta Formation (VMF) in the Neuquén Basin, Argentina.
- A core sample extracted at depth 3100 m was dried under laboratory conditions.
- Ultrasonic phase velocity measurements conducted at a frequency of 1 MHz, exhibited a clear **vertical transverse anisotropy (VTI)** behavior in the formation.
- VMF has a stratified microstructure, with clay platelets and **organic matter (mostly kerogen)** parallel or sub-parallel to bedding.

# Well in the VMF from where the core sample was extracted

Rock Physics simulations using core data to estimate the stiffness tensor in Vaca Muerta organic-rich mudrock

Juan E. Santos,



Minerals and its proportions in the VMF well. The core interval is indicated by red dots.

# Characterization of ultra-low permeability, organic-rich mudrock reservoirs. II

- VMF is assumed to consist of a periodic sequence of very thin horizontal layers where **Biot's theory in the diffusive frequency range** is applicable.
- To characterize the VTI stiffness coefficients  $p_{ij}$  of the equivalent VTI medium, numerical harmonic simulations—both compressional and shear—were performed on a representative synthetic rock model.
- The **model consists of a periodic sequence of two porous materials**, both of 6 percent porosity and permeability  $2.75 \cdot 10^{-18} \text{ m}^2$ .

## Characterization of ultra-low permeability, organic-rich mudrock reservoirs. III

- Material 1 is a complex, multiminerall assemblage composed of seven solid phases, including 23 percent of kerogen, which is treated as a solid mineral constituent.
- After estimating the bulk and shear moduli of the individual solid phases using a **generalized Krief's model**, and taking into account their volume fractions, **for Material 1 we get a frame bulk modulus of 29.19 GPa and a shear modulus of 17.78 GPa**, values that lie within the Hashin–Shtrikman bounds.
- Material 2 is composed entirely of pure kerogen with grain modulus 7 GPa, density 1400 kg/m<sup>3</sup>, frame modulus 1.29 GPa and shear modulus 0.36 GPa.

Tables 1 and 2 display the fluid and mineral physical properties used in the harmonic simulations.

**Table 1. Fluid properties.**

fluid	Bulk modulus (Pa)	Density (kg/m <sup>3</sup> )	Viscosity (Pa . s)
Air	1.01325d5	1.225d0	1.805d-5
Water	2.25d9	1000	0.001
Oil	0.57d9	700	0.01
Gas	0.022d9	78	0.000015

**Table 2. Mineralogical properties obtained from X-ray diffraction (XRD) analysis of core sample, used for Material 1 at an effective pressure of 17.23 MPa**

mineral	Bulk modulus (GPa)	shear modulus (GPa)	Density (kg/m <sup>3</sup> )	Proportions (%)
kerogen	7.0	2.	1400	23
Clay	25	9	2700	0.3727
Quartz	45	55	2700	0.1461
Calcite	80	40	2800	0.1068
Plagioclase	80	40	2800	0.0257
Dolomite	100	50	2900	0.0237
Pyrite	170	110	5000	0.035

## Computed VTI velocities using dry-core data

The harmonic simulations were performed on a dry, square sample with a side length of 2 mm, consisting of four repetitions of a **periodic sequence composed of 49 layers of Material 1 and one layer of Material 2 per period**. Each layer has a uniform thickness  $10^{-5}$  m. The computational domain was discretized using a  $200 \times 200$  mesh.

Table 3 summarizes the results of the VTI analysis, showing a good agreement between the simulated and laboratory-measured phase velocities, with relative errors remaining below 10 per cent.

**Table 3. Phase velocities computed, measured and error percentage.**

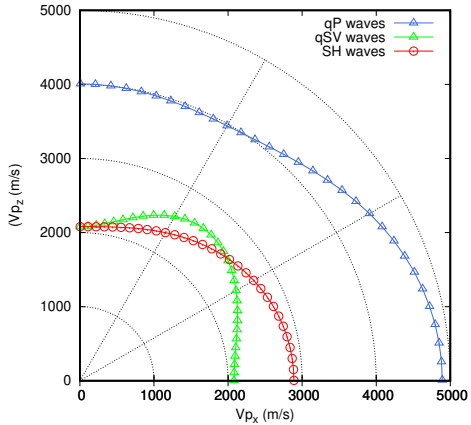
Phase velocity $v_p$ (m/s)	Computed	Measured	Percentage error
v11	4644.378	4331	7.2 %
v33	3804.510	4217.47	9.8 %
v55	1974.760	2193.61	9.9 %
v66	2742.641	2581	6.2 %

Figures 2 and 3 present polar plots of the phase and energy velocities, respectively, for the qP, qSV, and SH waves in the dry sample, computed using the FE method at a frequency of 1 MHz.

Rock Physics simulations using core data to estimate the stiffness tensor in Vaca Muerta organic-rich mudrock

Juan E. Santos,

# Polar representation of qP, qSV and SH phase velocities. Dry sample.



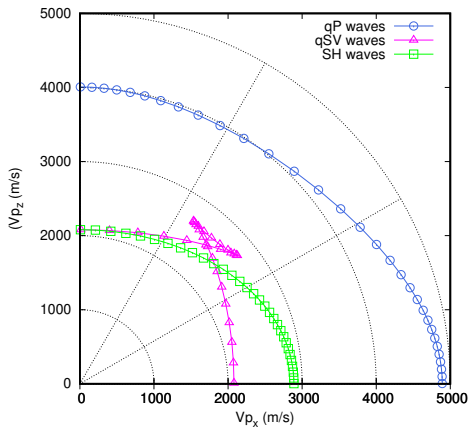
Polar representation of phase velocities of qP, qSV and SH waves computed using the FE method. Frequency is 1 MHz. 0 and 90 degrees indicate waves traveling parallel and normal to the bedding, respectively. Strong VTI behavior is observed.

# Polar representation of qP, qSV and SH energy velocities. Dry

sample.

Rock Physics  
simulations using  
core data to  
estimate the  
stiffness tensor in  
Vaca Muerta  
organic-rich  
mudrock

Juan E. Santos,

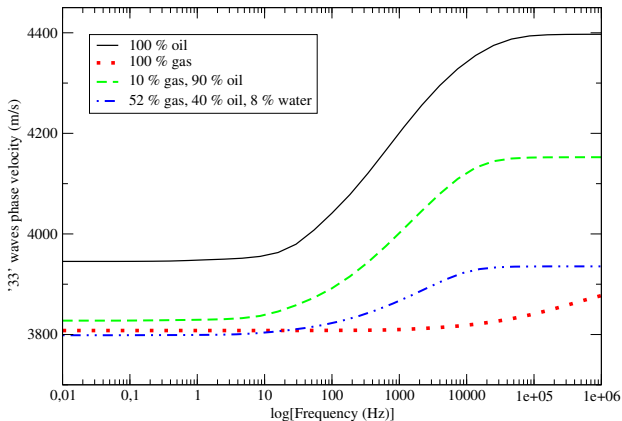


Polar representation of energy velocities of qP, qSV and SH waves computed using the FE method.

Frequency is 1 MHz. A notable triplication in the qSV-wave energy velocity pattern can be seen.

- Four fluid saturation scenarios are analyzed : 100 percent oil, 100 percent gas, 10 percent gas plus 90 percent oil and a ternary fluid mixture consisting of 40 percent gas, 52 percent oil, and 8 percent water, obtained from the well's fluid saturation log.
- the next Figures display phase velocities and attenuation factor  $1000/Q$ , with  $Q$  denoting the quality factor. We consider waves traveling normaly to the layering plane ('33' waves).
- For brevity, waves traveling parallel to the layering plane are not shown.
- While phase velocities allows to analyze velocity dispersion for the four saturation scenarios, the attenuation figure allows to study the WIFF.

# Phase velocity of '33' waves.

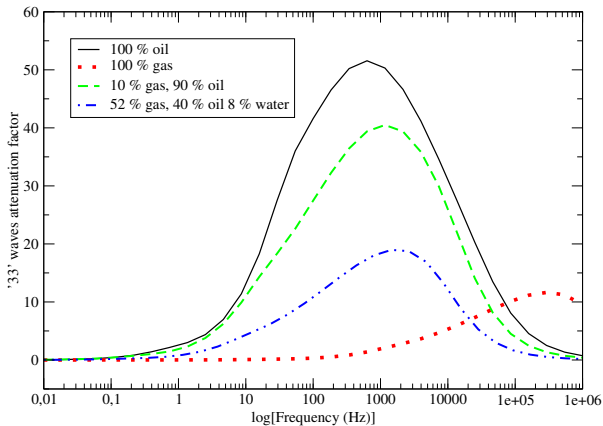


'33' waves phase velocity as function of frequency.

Rock Physics simulations using core data to estimate the stiffness tensor in Vaca Muerta organic-rich mudrock

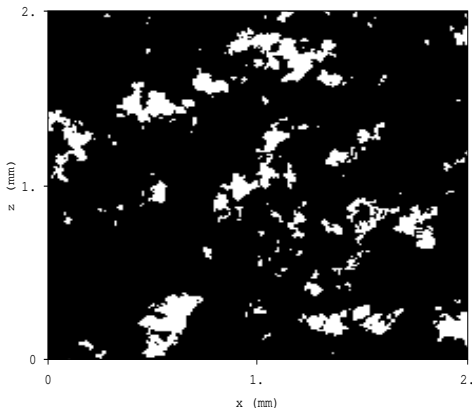
Juan E. Santos,

# Attenuation factor of '33' waves'



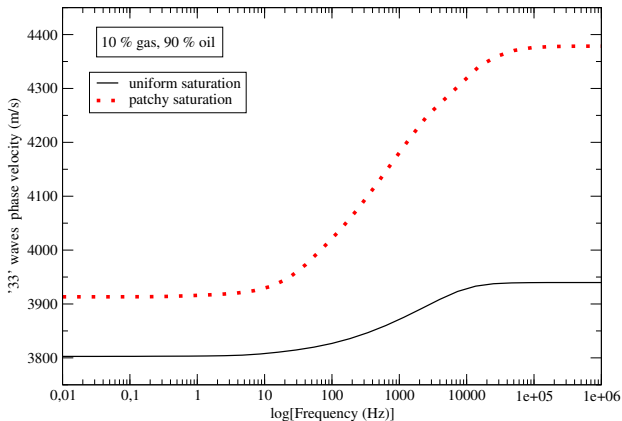
'33' waves phase attenuation factor as function of frequency.

The von Karman self-similar correlation function was used to generate patchy saturation patterns,



White zones correspond to full gas saturation and black regions to full oil saturation. Overall gas saturation is 10 percent.

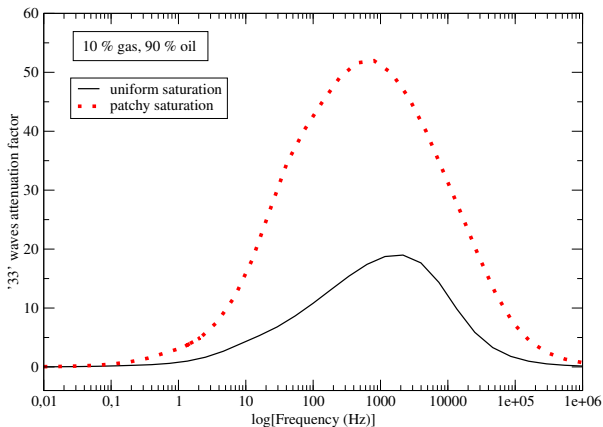
## Phase velocity of '33' waves for uniform and patchy saturation.



'33' phase velocity for uniform and patchy saturation as function of frequency.

# Attenuation factor of '33' waves for uniform and patchy saturation.

saturation.



'33' waves attenuation factor for uniform and patchy saturation as function of frequency.

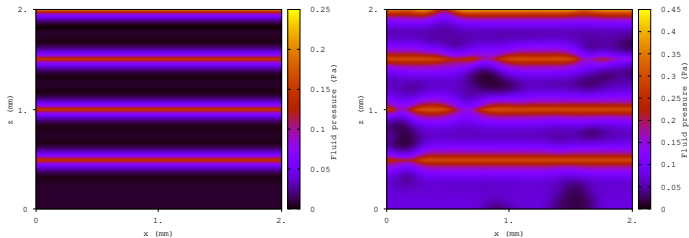
Rock Physics  
simulations using  
core data to  
estimate the  
stiffness tensor in  
Vaca Muerta  
organic-rich  
mudrock

Juan E. Santos,

Rock Physics  
simulations using  
core data to  
estimate the  
stiffness tensor in  
Vaca Muerta  
organic-rich  
mudrock

Juan E. Santos,

## Fluid pressure of '33' waves for uniform and patchy saturation.



Fluid pressure for the case of 10 % gas, 90 % oil and uniform (left) and patchy (right) saturation.

Frequency is 100 Hz

- This study presented a physically grounded, non-phenomenological methodology for estimating the effective anisotropic behavior of the organic-rich mudrock reservoirs.
- The simulations were performed on a finely layered synthetic medium representative of a core sample from the Vaca Muerta Formation.
- The computed stiffness tensors showed very good agreement with laboratory-measured phase velocities and well-log data, capturing the strong VTI anisotropy of the formation.
- The inclusion of both patchy and uniformly mixed fluid saturation scenarios emphasized the critical influence of mesoscale fluid heterogeneities on seismic wave dispersion and attenuation.